ADVANCED FUNCTIONAL MATERIALS
www.afm-journal.de

Highly Efficient Multifunctional Supramolecular Gene Carrier System Self-Assembled from Redox-Sensitive and Zwitterionic Polymer Blocks

*Yuting Wen, Zhongxing Zhang, and Jun Li**

It has been a challenge to incorporate multiple features into a single gene carrier system to overcome numerous hurdles during the gene delivery. Herein, a supramolecular approach for building a multifunctional gene carrier system is demonstrated with the functions of disulfide bond based reduction-responsive degradation and zwitterionic phosphorylcholine based extracellular stabilization and favorable cellular uptake. The gene carrier system is self-assembled from two molecular building blocks: one host polymer, which is a redox-sensitive β-cyclodextrin based cationic star polymer, and one guest polymer, which is adamantyl end capped zwitterionic phosphorylcholine based polymer. The host and guest polymers self-assemble to integrate multiple functions into one system, based on the host-guest interaction between β-cyclodextrin and adamantyl moieties. With the rational designs of both building blocks, the supramolecular gene carrier system possesses excellent protein stability, serum tolerance, cellular uptake and intracellular DNA release properties, and also low cytotoxicity. These features work simultaneously to achieve exceptionally high gene transfection efficiency, which is proven in MCF-7 cell cultures using luciferase and green fluorescence protein reporter genes. Finally, the supramolecular gene carrier is applied to deliver the therapeutic p53 anti-cancer gene in MCF-7 cells, showing great potential for cancer gene therapy application.

1. Introduction

Gene delivery holds great promises as a therapeutic approach for many diseases such as cancers, genetic disorders and acquired diseases. Cationic polymers are a major type of non-viral gene vectors with an attractive feature that they can be tailored and synthesized to meet the requirements for different gene delivery processes.[1,2] Various cationic polymers such as polyethylenimine (PEI), poly-L-lysine (PLL), and poly(2-dimethylaminoethyl methacrylate) (pDMAEMA) have been extensively investigated as versatile gene carriers.[3] Such cationic polymers can compact nucleic acids to form polyplex nanoparticles, which can protect them from extracellular enzymatic degradation, and enter cells via endocytosis followed by releasing the genes inside the cytoplasm or nucleus of the cells.[4] However, low gene transfection efficiency is a common disadvantage of these polymeric systems due to the multiple hurdles during the gene delivery processes such as low stability during extracellular transport, inefficient cellular internalization, slow endosomal escape, unpacking and release of gene, poor nuclear translocation, and potential cytotoxicity.

Although methodologies are existing or under development for solving individual barriers in the polymeric gene delivery processes, it is eventually a big challenge to design a multifunctional polymeric system with multiple features incorporated and optimized to overcome these hurdles collectively to achieve a highly efficient and safe gene delivery.[5,6] For example, to incorporate bioreducible disulfide linkages in polymer chains can make the gene delivery system respond to the intracellular reductive environment, and then achieve well-balanced extracellular protection and intracellular release of genes. The disulfide bond is prone to rapid cleavage in the cytosol that is a reductive environment with glutathione level up to 0.5–10 mM, but remains stable in extracellular environment with glutathione level at 2–20 μM.[7–10] As another example, to conjugate poly(2-methacryloyloxyethyl phosphorylcholine) (pMPC) to a gene carrier can sterically inhibit protein adsorption and enhance serum tolerance of the gene vector,[11,12] while the zwitterionic pMPC mimics the surface of natural phospholipid bilayer membranes, and may facilitate cellular association and enhance cellular uptake.[13–15]

Y. Wen, Prof. J. Li
Department of Biomedical Engineering
Faculty of Engineering
National University of Singapore
7 Engineering Drive 1, Singapore 117574, Singapore
E-mail: jun-li@nus.edu.sg; bielj@nus.edu.sg
Dr. Z. Zhang, Prof. J. Li
Institute of Materials Research and Engineering
A*STAR (Agency for Science
Technology and Research)
3 Research Link, Singapore 117602, Singapore
Prof. J. Li
NUS Graduate School for Integrative Sciences & Engineering (NGS)
National University of Singapore
28 Medical Drive, Singapore 117456, Singapore

DOI: 10.1002/adfm.201303687

Supramolecular chemistry has offered a powerful and convenient method for fabricating complicated nanostructures self-assembled from individually tunable molecular building blocks. Various self-assembly approaches such as multilayered assembly and complementary DNA strand self-assembly have been reported for building multifunctional gene delivery systems.[16–20] β-Cyclodextrin (β-CD) and adamantane (Ad) form a pair of host and guest molecules that self-assemble to give an inclusion complex with high affinity.[21] Researchers including us have demonstrated several supramolecular polymers formed through inclusion complexation based on non-covalent host-guest interaction between β-CD and adamantyl moieties, for soft materials and biomaterials applications.[22–30] The use of β-CD provided not only the host moiety for building the supramolecular assembly structure, but also a core for designing functional strictures such as star-shaped polymers. Therefore, the β-CD based polymers could be complexed with adamantyl-based polymers that carry additional functional components. Compared to traditional covalent conjugation approach, this supramolecular approach is more convenient in building complicated architectures with multiple functionalities integrated within one system.

Herein, we demonstrate a prototype of such supramolecular self-assembly architectures as a multifunctional gene carrier system with the functions of disulfide bond based reduction-responsive degradation and zwitterionic phosphorylcholine based extracellular stabilization and favorable cellular uptake for delivering DNA with significantly enhanced gene transfection efficiency. This delivery system is composed of two molecular building blocks: one host polymer and one guest polymer, which can self-assemble to integrate multiple functions into one carrier system, based on the host-guest interaction between β-CD and adamantyl (Ad) moieties in the host and guest, respectively. The host polymer is a star-shaped cationic polymer with multiple arms of pDMAEMA linked to a β-CD core with bioreducible disulfide bonds (βCD-SS-pDMAEMA, and further shortened to βCD-SS-P). The guest polymer is an adamantyl end capped pMPC (Ad-pMPC). Therefore, βCD-SS-P and Ad-pMPC could self-assemble to form a supramolecular pseudo-diblock copolymer (βCD-SS-P/Ad-pMPC), which can further compact DNA to form polyplex nanoparticles with pMPC as the corona (**Figure 1**). This design is expected to provide the polyplex nanoparticles with high extracellular stability and protein resistance due to the shielding effect of pMPC, as well as high efficiency of cellular internalization due to the membrane-mimic structure of pMPC. Once internalized into the cytoplasm, the payload DNA can be readily released because the disulfide bonds can be cleaved by the intracellular reductive environment. In this study, the βCD-SS-P/Ad-pMPC/DNA polyplex system was systematically investigated in comparison with control systems such as non-bioreducible, and non-shielding or PEG shielding DNA polyplexes. It was revealed that the protein stability, serum tolerance, cellular uptake, and intracellular release of DNA were all greatly enhanced by the novel design, resulting in a highly efficient gene delivery system. Furthermore, the excellent gene delivery ability of the βCD-SS-P/Ad-pMPC assembly was applied for delivering the therapeutic p53 anti-cancer gene with great efficiency.

2. Results and Discussion

2.1. Formation of βCD-SS-P/Ad-pMPC Supramolecular Pseudo-Diblock Copolymer

For synthesis of βCD-SS-P, disulfide linkages were first introduced to β-CD to give βCD-SS-NH_2, followed by reaction with a-bromoisobutyric acid to produce βCD-SS-Br as the ATRP macroinitiator. Then βCD-SS-P star-shaped polymer, consisting of β-CD core and pDMAEMA arms linked by disulfide bonds, was subsequently prepared via ATRP of DMAEMA monomer. It was determined that there were 4 arms of pDMAEMA attached to the β-CD core, and the degree of polymerization (DP) of total 4 arms of pDMAEMA was 58. For synthesis of Ad-pMPC, the ATRP initiator bromoisobutyryl-terminated adamantane (Ad-Br) was first synthesized. Then, the Ad-pMPC zwitterionic polymer was subsequently prepared via ATRP of MPC monomer. The DP of Ad-pMPC was determined to be 18. The details of the synthesis procedures are described in Supporting Information, and the NMR spectroscopic characterization and elemental analysis data are shown in Supporting Information Figures S1,S2 and Tables S1,S2.

The βCD-SS-P/Ad-pMPC supramolecular pseudo-diblock copolymer was formed by mixing the host and guest polymers at 1:1 molar ratio in aqueous solution. The GPC analyses were performed for βCD-SS-P/Ad-pMPC supramolecular copolymer in comparison with βCD-SS-P, Ad-pMPC, and the βCD-SS-P/pMPC physical mixture, where pMPC is a control polymer without adamantyl end cap (**Figure 2**A). The GPC diagram of the βCD-SS-P/Ad-pMPC supramolecular copolymer showed one unimodal elution peak, while two peaks were observed for the βCD-SS-P/pMPC physical mixture. The βCD-SS-P/Ad-pMPC supramolecular copolymer gave higher MW (M_n = 12.9 kDa, M_w/M_n = 1.12) than either βCD-SS-P host star polymer (M_n = 9.1 kDa, M_w/M_n = 1.13) or Ad-pMPC guest polymer (M_n = 4.9 kDa, M_w/M_n = 1.18), suggesting that βCD-SS-P and Ad-pMPC were self-assembled through inclusion complexation between β-CD and Ad moieties.

To further confirm the formation of βCD-SS-P/Ad-pMPC supramolecular copolymer, 1:1 inclusion complex of βCD-SS-P and Ad-pMPC in D_2O was studied by 2D-NOESY NMR spectroscopy (Figure 2B). A series of NOE cross peaks between the inner protons of C(3)H and C(5)H of β-CD and the methane (H_b) and methylene (H_c) protons of the Ad were observed. The results indicate that the adamantyl moiety entered into the hydrophobic cavity of β-CD to form the host-guest inclusion complex. No intermolecular NOE interaction between the Ha proton of Ad and the protons of the β-CD torus could be found in the spectrum, indicating that the adamantyl group entered β-CD core from the wide side of β-CD, but not from the narrow side. Thus, the NMR spectroscopic studies gave clear evidence that the supramolecular pseudo-diblock copolymer was formed via host-guest inclusion complexation between the β-CD core and the adamantyl unit.

In order to test the biodegradation of the βCD-SS-P/Ad-pMPC supramolecular copolymer, the samples were incubated in PBS with and without the reducing agent dithiothreitol (DTT) that simulates the intracellular redox-potentials, and

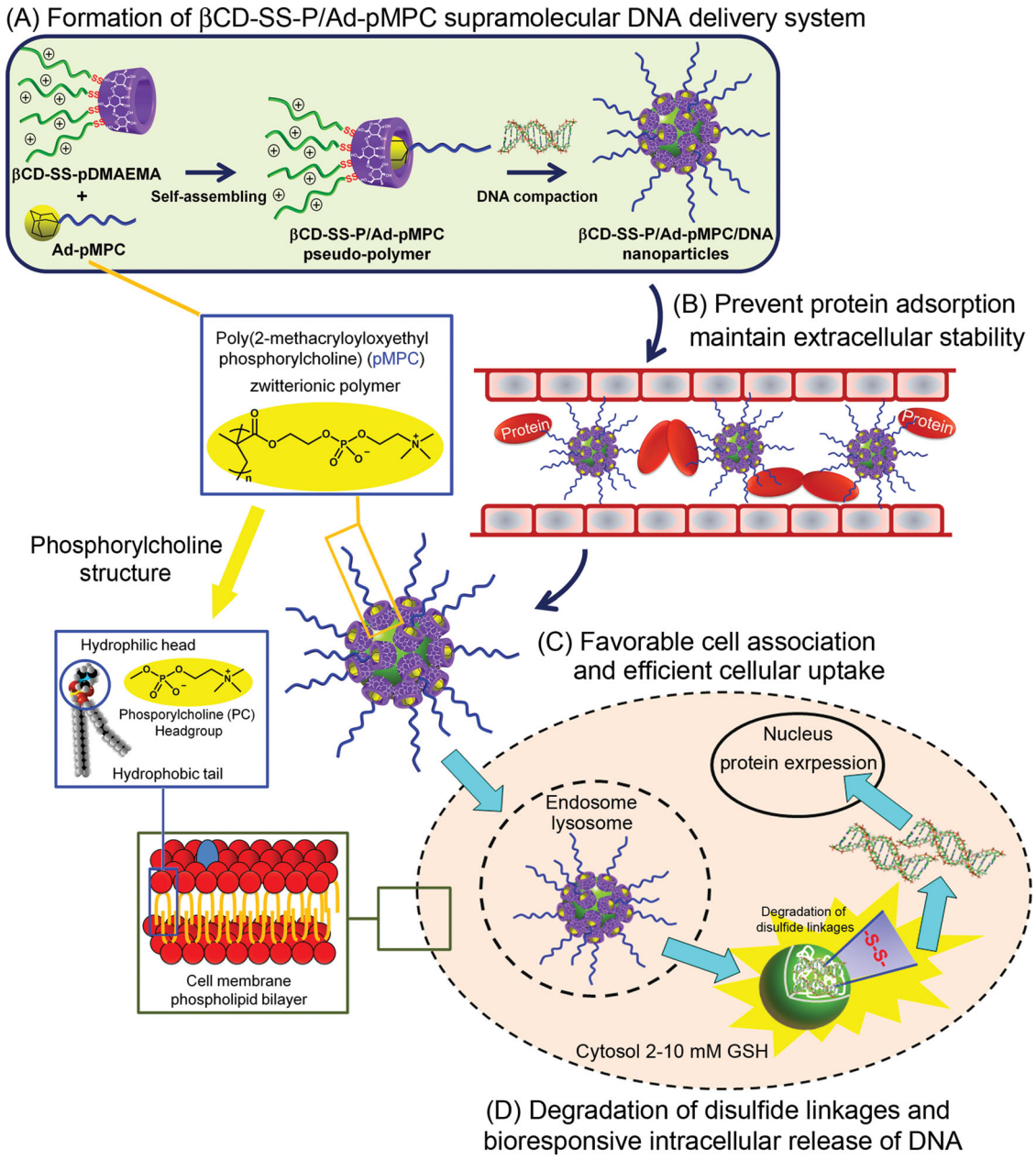

Figure 1. Conceptual illustration of the βCD-SS-P/Ad-pMPC supramolecular gene delivery system. A) Formation of βCD-SS-P/Ad-pMPC pseudo-diblock copolymer via host-guest interaction, followed by DNA compaction to form βCD-SS-P/Ad-pMPC/DNA polyplex. B) The protein-repellent properties of pMPC imparting the extracellular stability of the polyplex. C) Favorable cellular association and efficient cellular uptake due to the zwitterionic phosphorylcholine structure of pMPC corona. D) Rapid intracellular unpacking and release of DNA owing to the redox-sensitive disulfide linkages followed by efficient gene transfection.

the degradation was monitored by GPC (Figure 2C). After 4 h DTT treatment, a series of lower MW peaks were observed and the polydispersity increased significantly. In contrast, the MW of the supramolecular polymer did not change at all under the non-reducing environment in PBS. The results indicate that the βCD-SS-P/Ad-pMPC supramolecular copolymer is degradable under the reducing conditions, while physiological ionic strength will not affect its MW. This redox-sensitive biodegradation property is crucial to the in vivo application of the gene carrier.

Further, the βCD-SS-P/Ad-pMPC supramolecular copolymer had good DNA binding ability, forming DNA polyplex nanoparticles with sizes ranging from 110 to 150 nm and zeta potential values ranging from 18 to 25 mV when N/P ratios were 10 to 40 (N/P ratio is the molar ratio of nitrogen residues of cationic polymer to phosphate groups of DNA). Transmission electron microscopy (TEM) observation showed that morphology of βCD-SS-P/Ad-pMPC/DNA polyplexes (N/P = 20) were compact and spherical, with sizes less than 200 nm (Supporting Information Figure S3).

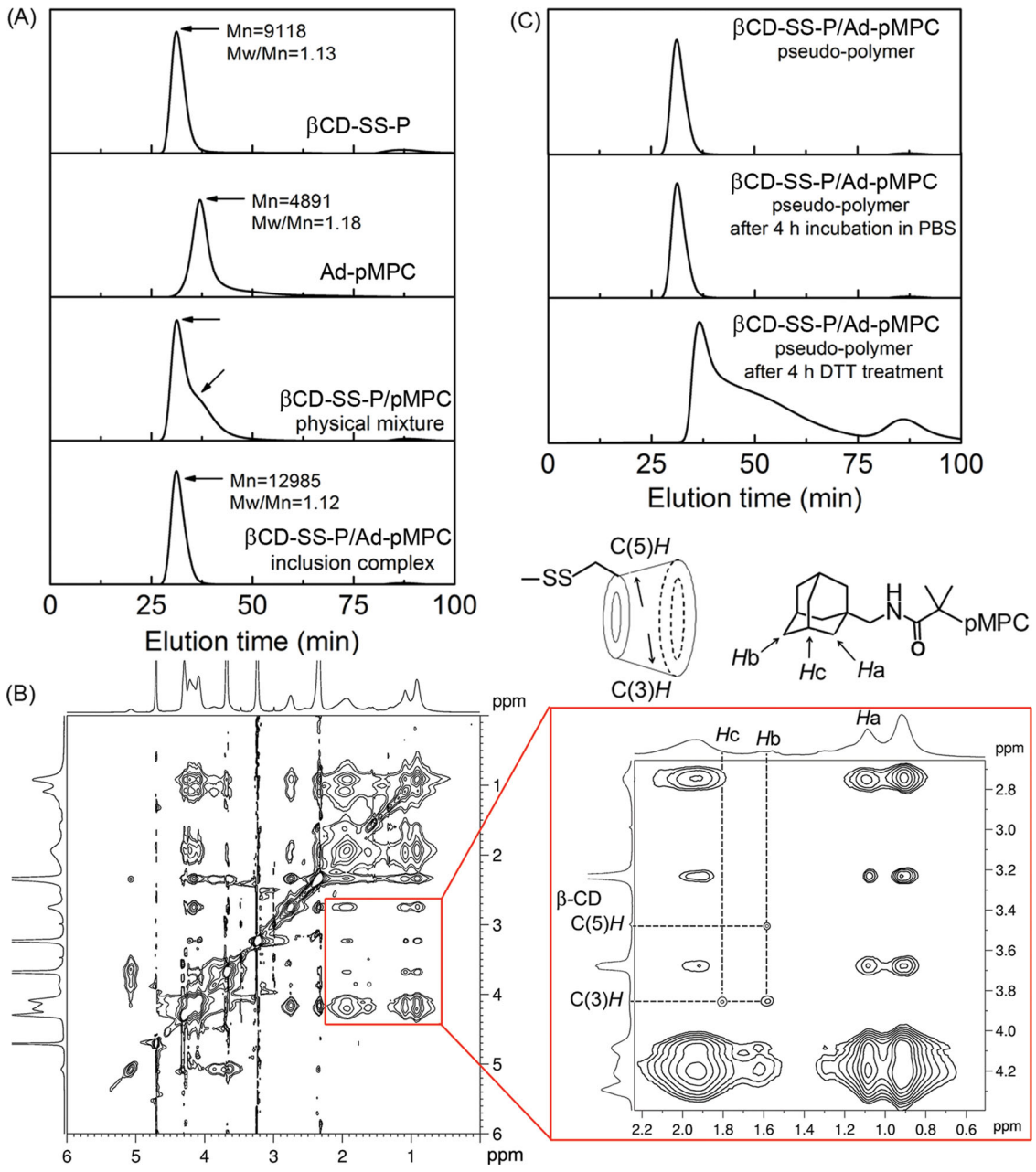

Figure 2. Formation of βCD-SS-P/Ad-pMPC supramolecular pseudo-diblock copolymer. A) Representative GPC traces obtained for βCD-SS-P, Ad-pMPC, physical mixture of βCD-SS-P and pMPC at 1:1 molar ratio (the degree of polymerization of pMPC was the same as Ad-pMPC), and inclusion complex of βCD-SS-P/Ad-pMPC at 1:1 molar ratio. B) 2D-NOESY NMR spectra of the 1:1 host-guest inclusion complex of βCD-SS-P and Ad-pMPC in D_2O (300 MHz). Left: full scale; and right: scale-up of selected area. C) GPC traces of CD-SS-P/Ad-pMPC supramolecular copolymer after incubation in PBS without and with DTT (20 mM) for 4 h at 37 °C.

2.2. Effect of Disulfide Bond on Intracellular Release, Cytotoxicity, and Gene Transfection

Prior to investigating the effect of disulfide bond on intracellular release of DNA, we demonstrated that the βCD-SS-P/Ad-pMPC/DNA polyplex nanoparticles were stable and DNA was well protected in saline solution, while the deshielding, polyplex dissociation, and DNA release took place rapidly in a solution with DTT (20 mM) that simulates the reductive condition in the cytoplasm (Supporting Information Figure S4).

The intracellular degradation of βCD-SS-P/Ad-pMPC/DNA polyplexes and release of DNA were traced by observing the intracellular trafficking of fluorescence labeled βCD-SS-P/Ad-pMPC/DNA nanoparticles using CLSM at various time points (**Figure 3**A). The colocalization of FITC-labeled polymer βCD-SS-P/Ad-pMPC (green) and rhodamine-labeled DNA (red) would produce a yellow fluorescence in merged images.

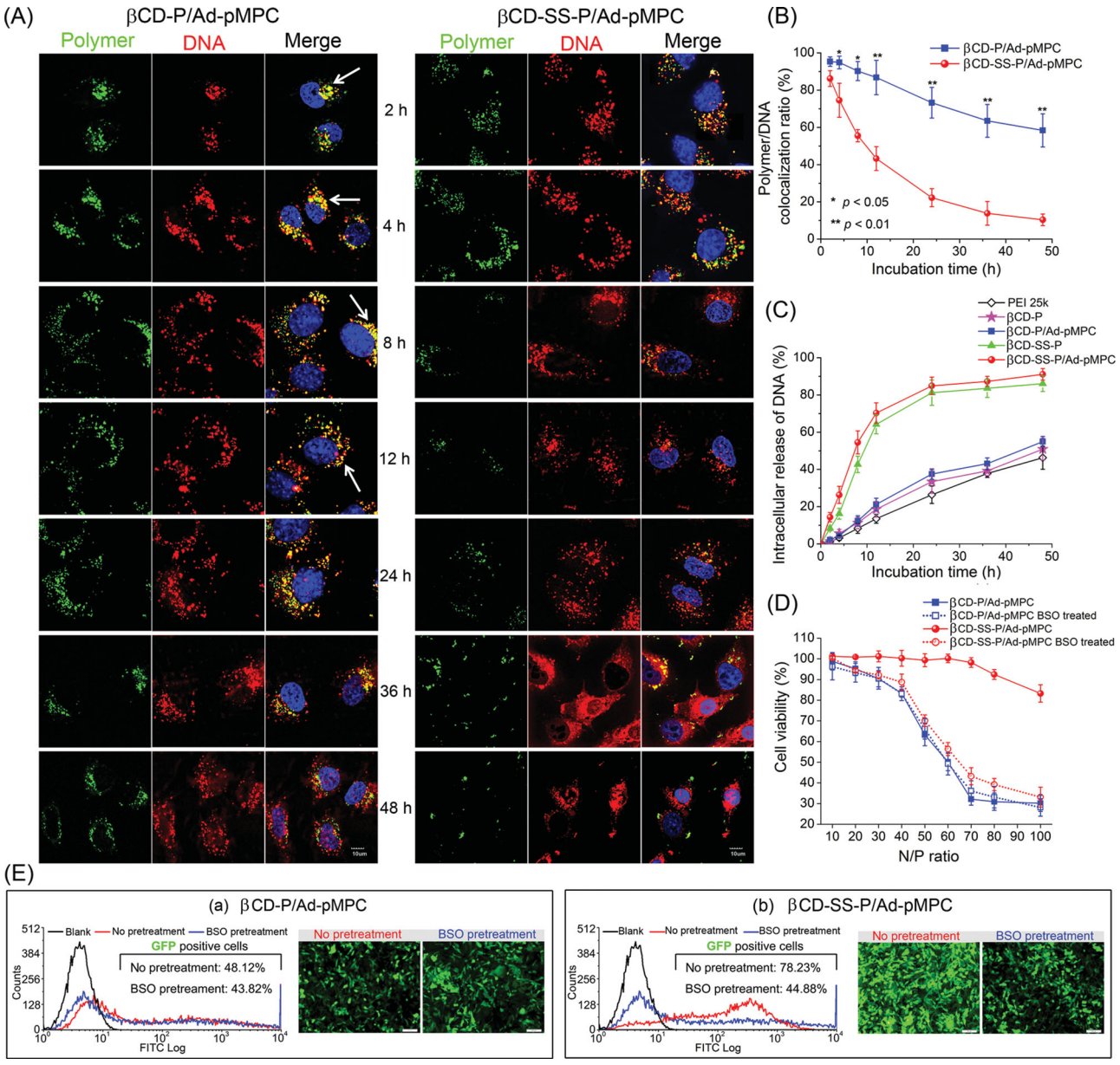

Figure 3. Effects of disulfide linkages of βCD-SS-P/Ad-pMPC/DNA polyplex system on intracellular DNA release, cytotoxicity, and gene transfection. A) Confocal microscope images showing cellular distribution of FITC-labeled polymers (green) and CX-rhodamine-labeled DNA (red) in MCF-7 cells at different time points post transfection. FITC fluorescence dye was labeled to the hydroxyl groups of β-CD of the host polymer. Cell nuclei were stained with DAPI (blue). Colocalization of DNA and polymer appeared yellow in merged images, indicating DNA was bound with cationic polymer. Scale bar is 10 μm. B) Ratio of colocalization of CX-rhodamine-labeled DNA and FITC-labeled polymer at various time points calculated from the number of pixels using ImageJ. Data represent means ± S.D. for 20 cells (*$p < 0.05$, **$p < 0.01$). C) Cumulative intracellular release of DNA (the percentage of released DNA of all internalized DNA) at various time points measured by PicoGreen assay after cell lysis. Data represent means ± S.D. ($n = 3$). D) Cytotoxicity of βCD-SS-P/Ad-pMPC/DNA and other control polyplexes in MCF-7 cells pre-treated without and with BSO (500 μM). BSO was used to deplete intracellular GSH. E) GFP transfection using pEGFP-N1 mediated by a) βCD-P/Ad-pMPC and b) βCD-SS-P/Ad-pMPC complexes in MCF-7 cells pre-treated without and with BSO (Left panel: Flow cytometric histograms of GFP-transfected cells. Black line: cells without GFP transfection; Red line: cells with GFP transfection but without BSO pre-treatment; Blue line: cells with GFP transfection and BSO pre-treatment. Right panel: Fluorescence microscopy images of cells with GFP transfection; Scale bar is 100 μm).

Otherwise, if the DNA is released from the polyplex, the green signals of FITC-polymer and the red signals of rhodamine-labeled DNA would appear separately. For non-degradable control system βCD-P/Ad-pMPC, even after 12 h incubation, there were still a large number of yellow dots (marked by white arrows) distributed within the cytoplasm in the merged images, produced by the colocalization of FITC-βCD-P and rhodamine-DNA, indicating that the release of DNA was very slow. In contrast, for the redox-responsive system βCD-SS-P/Ad-pMPC, the number of red dots increased and the yellow dots

decreased quickly in the merged images, indicating that DNA was rapidly released due to the dissociation of the polyplex with the cleavage of the disulfide linkages. Moreover, the area of green pixels decreased with time, which may be a result of the removing of the β-CD fragments (β-CD was FITC-labeled) from the cells after the degradation.

The polymer-DNA colocalization ratio is plotted against incubation time (Figure 3B). For the non-degradable control system βCD-P/Ad-pMPC, the colocalization ratio remained very high after a long incubation time, being 86.8% at 12 h, and even 58.4% at 48 h. However, for the redox-responsive system βCD-SS-P/Ad-pMPC, the colocalization ratio decreased quickly to 43.5% at 12 h and 10.4% at 48 h, which was significantly lower than that of non-degradable system.

The kinetics of the intracellular release of DNA was further quantitatively studied by using PicoGreen assay. The percentage of released DNA of all internalized DNA at various time points is shown in Figure 3C for a few carrier systems. The unpacking and release of internalized DNA from all non-degradable carrier systems occurred in a slow manner over the course of 48 h. The cumulative release of DNA at 24 h was only 26.4%, 33.4%, and 37.5% for PEI 25 k, βCD-P, and βCD-P/Ad-pMPC, respectively. In contrast, the release of DNA from both redox-sensitive βCD-SS-P and βCD-SS-P/Ad-pMPC polyplexes was marked by a burst release within the first 12 h, due to the cleavage of the disulfide linkages within the cells. The cumulative release of DNA at 24 h was 81.2% and 84.9% for the two redox-sensitive carrier systems, respectively. The results suggest that the βCD-SS-P/Ad-pMPC/DNA polyplex exhibited not only rapid, but also complete release of internalized DNA within the cells.

The cytotoxicity of βCD-SS-P/Ad-pMPC on MCF-7 cells was significantly lower than that of non-degradable PEI 25 k and βCD-P carriers in the forms of both polymer alone and DNA polyplex (Supporting Information Figure S5). To examine whether the improved cytotoxicity profile of βCD-SS-P/Ad-pMPC was ascribed to the cleavage of the disulfide bonds that is associated with the intracellular glutathione (GSH) levels, the cytotoxicity of the polymers was further evaluated in the cells treated with and without D,L-buthionine sulfoximine (BSO).[31] BSO is known as GSH inhibitor, leading to depletion of intracellular GSH. It is believed that no intracellular cleavage of disulfide linkages will occur once the GSH is depleted. As shown in Figure 3D, it was clearly observed that the depletion of intracellular GSH by BSO led to significant elevation of cytotoxicity of the redox-responsive system βCD-SS-P/Ad-pMPC, approximately up to the level of its non-degradable analogue βCD-P/Ad-pMPC. As expected, non-degradable βCD-P/Ad-pMPC did not show such cytotoxicity dependence on the GSH level. Thus, it is proved that the intracellular degradation of the βCD-SS-P/Ad-pMPC pseudo-copolymer contributed to the low cytotoxicity.

The gene transfection efficiency of the gene carriers was evaluated by luciferase and green fluorescence protein expression using pRL-CMV and pEGFP-N1 plasmids. The luciferase gene transfection efficiency of βCD-SS-P was 4 to 30 folds higher than that of PEI 25 k and βCD-P controls (Supporting Information Figure S6). Similarly, βCD-SS-P/Ad-pMPC showed much higher GFP gene transfection efficiency than βCD-P/Ad-pMPC (Figure 3E). The gene transfection experiments were done in MCF-7 cells pre-treated without and with BSO, thereby the transfection efficiency under normal and low GSH levels was compared. For the non-degradable βCD-P/Ad-pMPC, the GFP positive cell counts were 48% (without BSO treatment) and 44% (with BSO treatment). In such case, the gene transfection efficiency was not affected by the treatment of BSO. For βCD-SS-P/Ad-pMPC, the GFP positive cell counts were 78% (without BSO treatment) and 45% (with BSO treatment). As expected, the depletion of intracellular GSH led to much lower protein expression level. These results confirmed that the intracellular cleavage of disulfide linkages of βCD-SS-P/Ad-pMPC polyplexe and thereby the rapid DNA release did play a crucial role in improving the gene transfection efficiency.

2.3. Serum Stability of βCD-SS-P/Ad-pMPC/DNA Polyplex Nanoparticles

It is known that gene transfection efficiency is significantly reduced by presence of serum for most of cationic polymer gene delivery systems.[32] In this study, one of the purposes to introduce Ad-pMPC zwitterionic polymer block was to enhance the serum tolerance of the gene delivery system. The dynamic light scattering (DLS) and protein adsorption measurements showed that the shielding of pMPC block prevented the aggregation of the βCD-SS-P/Ad-pMPC/DNA polyplex nanoparticles and also greatly suppressed the protein adsorption of the polyplex nanoparticles (Supporting Information Figure S7).

Here, the effect of pMPC decoration on serum tolerance was investigated in MCF-7 cell culture system (**Figure 4**). The presence of serum significantly reduced the luciferase expression of Lipofectamine 2000, PEI 25k, βCD-P, and βCD-SS-P (Figure 4A). All these non-shielding vector systems suffered at least 10^3 times reduction in transfection efficiency in the presence of 50% FBS as compared to the serum free condition. However, the βCD-SS-P/Ad-pMPC system exhibited very stable transfection levels at various FBS concentrations. At 50% serum concentration, it still maintained 35% transfection efficiency as compared to that under serum free condition. On the other hand, at 50% serum concentration, βCD-SS-P/Ad-pMPC system showed 10^3 times higher luciferase expression than βCD-SS-P alone, suggesting that the zwitterionic Ad-pMPC shell greatly improved the serum tolerance of the gene delivery system.

Flow cytometry and confocal microscope were employed to measure the cellular uptake of the polyplex nanoparticles formed by CX-rhodamine-labeled DNA and βCD-SS-P/Ad-pMPC at different serum concentration levels, in comparison with the non-pMPC modified control. Figure 4B displays the flow cytometry histograms, from which the fluorescence intensity of cells and the relative number of cells internalized with CX-rhodamine labeled DNA were obtained at different serum concentration levels (Figure 4C). For non-pMPC modified βCD-SS-P, the presence of serum significantly decreased the fluorescence intensity of the cells as well as the relative DNA-positive cell number, indicating a significant decrease in cellular uptake efficiency of the polyplex nanoparticles. However, the cellular uptake efficiency for βCD-SS-P/Ad-pMPC polyplex nanoparticles showed nearly no changes with the increase in serum

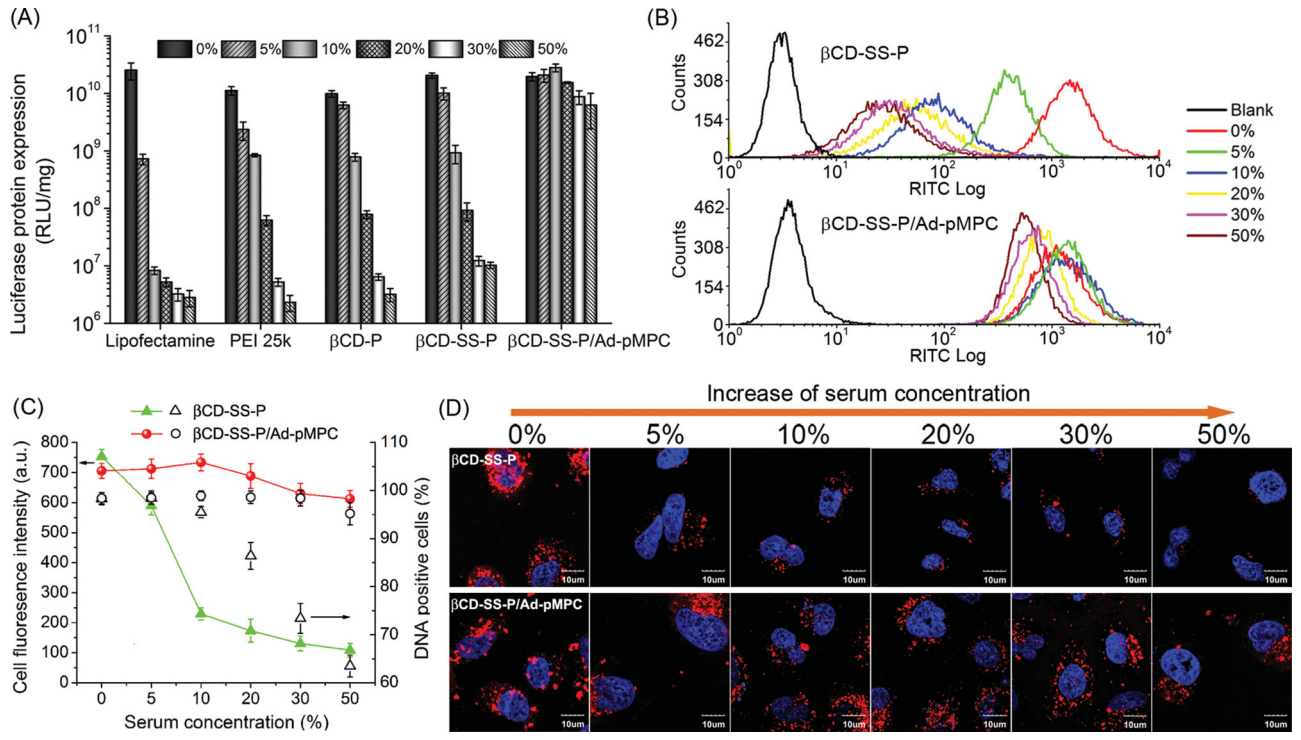

Figure 4. Evaluations of serum-tolerance of βCD-SS-P/Ad-pMPC/DNA system in MCF-7 cell culture with various serum concentrations. A) Gene transfection efficiency of βCD-SS-P/Ad-pMPC/DNA polyplex. Non-pMPC systems were used as controls. Data represent mean ± S.D. ($n = 3$). B) Flow cytometric analysis for cellular internalization of polyplex nanoparticles. CX-rhodamine labeled DNA was used. C) Gated mean fluorescence intensity (MFI) of cells (solid dots + lines) and relative number of cells with CX-rhodamine labeled DNA internalized (empty dots without lines) measured by flow cytometry after 4 h of incubation with polyplex nanoparticles. Data represent mean ± S.D. ($n = 3$). D) Confocal microscopic images of MCF-7 cells after 4 h of incubation with polyplexes containing 0.5 μg of CX-rhodamine-labeled DNA (N/P ratio = 20). Scale bar: 10 μm.

concentration. In addition, similar trends were observed by confocal microscope (Figure 4D). For the βCD-SS-P system, the increase in serum concentration caused significant decrease in red color dots, corresponding to the decrease in CX-rhodamine labeled DNA concentration in the cells. However, for the βCD-SS-P/Ad-pMPC system, the CX-rhodamine labeled DNA concentration in the cells showed no clear changes with increase in the serum concentration. Evidently, βCD-SS-P/Ad-pMPC polyplex nanoparticles showed significantly high cellular uptake efficiency at high serum concentrations, which was due to the pMPC shell that provided shielding and stability for the polyplex nanoparticles against serum.

2.4. Enhanced Cellular Uptake of βCD-SS-P/Ad-pMPC/DNA Polyplex Nanoparticles

In this study, the zwitterionic phosphorylcholine based pMPC, instead of traditional PEG shielding shell, was introduced to the redox-sensitive supramolecular polyplex nanoparticles. We hypothesize that the phosphorylcholine-based pMPC could strongly associate with the cell surfaces due to its membrane-mimetic structure.

The cellular uptake of DNA polyplexes formed by βCD-SS-P/Ad-pMPC and βCD-SS-P/Ad-pEG was compared. It is noted that the βCD-SS-P/Ad-pEG pseudo-copolymer was prepared using the same βCD-SS-P host polymer, and the length of Ad-pEG was the same as Ad-pMPC. The zeta potential values of both polyplexes were also similar. The kinetics of cellular uptake of polyplexes of CX-rhodamine-labeled DNA with βCD-SS-P/Ad-pMPC and βCD-SS-P/Ad-pEG in MCF-7 cells was studied with flow cytometry (**Figure 5**A). The relative DNA-positive cell number and the MFI per cell obtained from the flow cytometic histograms are plotted against incubation time (Figure 5B,C). It is clear that the cellular uptake for βCD-SS-P/Ad-pMPC polyplex was much more rapid and efficient than βCD-SS-P/Ad-pEG. For βCD-SS-P/Ad-pMPC polyplex system, with only one hour incubation 80% of the MCF-7 cells had taken up the nanoparticles. In contrast, for βCD-SS-P/Ad-pEG polyplex, it took up to 8 h to achieve 80% cellular uptake. In addition, all the MFI values of βCD-SS-P/Ad-pMPC systems were significantly higher than those of βCD-SS-P/Ad-pEG (after 1 h incubation, $p < 0.01$). The huge difference of the cellular uptake kinetics implied that the zwitterionic pMPC corona exhibited favorable interactions with cell surface membranes. However, PEG could not interact with the cellular membranes and consequently displayed a much slower rate of cellular uptake.[33] The confocal microscope images also gave the same results (Figure 5D). The βCD-SS-P/Ad-pMPC system showed rapid cellular uptake due to the zwitterionic phosphorylcholine structure of pMPC.

In polymeric gene delivery, positively charged polyplexes would electrostatically interact and aggregate with serum proteins and other negatively charged biomolecules in the blood,

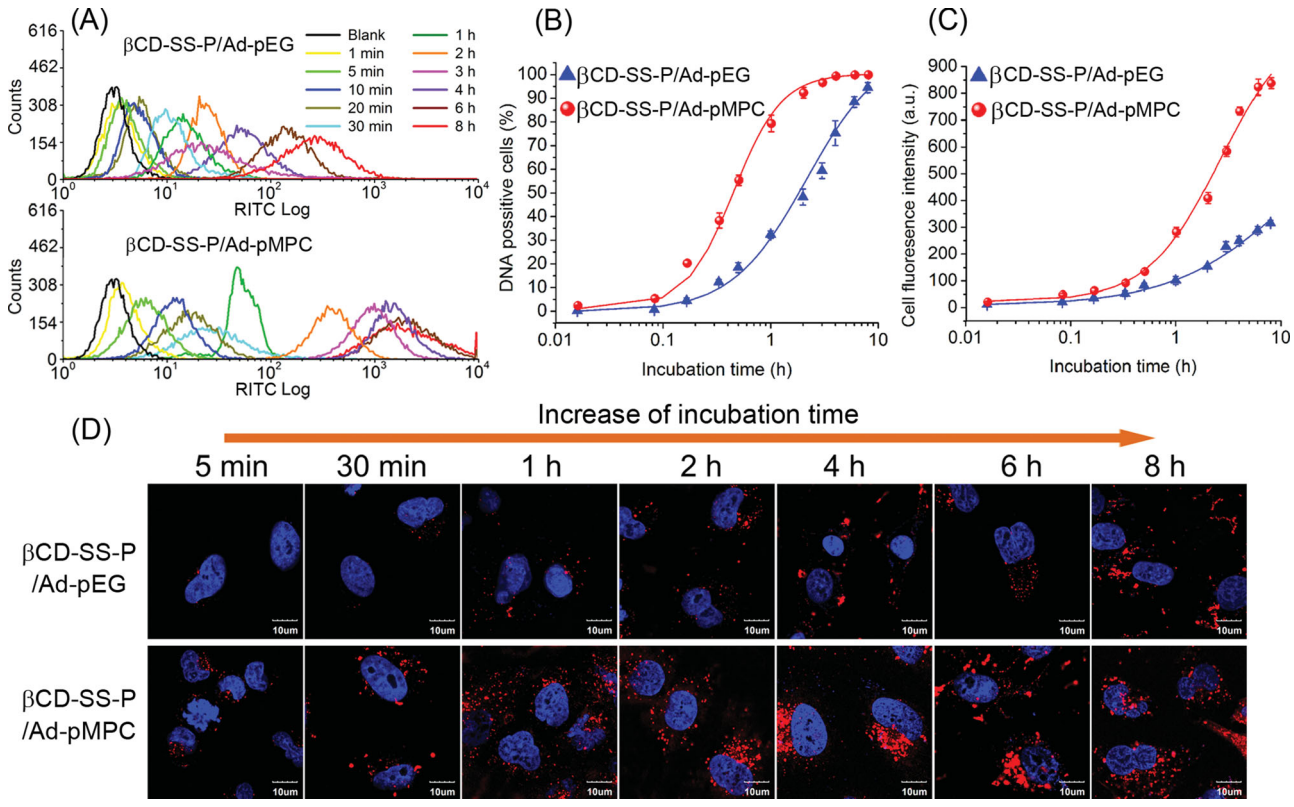

Figure 5. Cellular uptake kinetics for CX-rhodamine-labeled DNA polyplexes formed with βCD-SS-P/Ad-pEG and βCD-SS-P/Ad-pMPC pseudo-copolymers in MCF-7 cells. A) Flow cytometric histograms of MCF-7 cells after different times of incubation with the polyplexes. B) Relative number of fluorescence positive cells as a function of incubation time. C) Mean fluorescence intensity per cell as a function of incubation time. D) Confocal microscopic images of MCF-7 cells that internalized polyplexes containing 0.5 μg of CX-rhodamine-labeled DNA (N/P ratio = 20) at various incubation times (Scale bar = 10 μm).

limiting the blood circulation retention time of the polyplexes. Surface modification of polycations with hydrophilic PEG has become a widely used strategy to sterically inhibit protein adsorption and then enhance serum tolerance of gene vectors. However, PEG shielding has been demonstrated to lower the gene transfection efficiency due to the reduced cell-surface association and cellular uptake,[34–36] causing a "shielding dilemma". In contrast, the zwitterionic phosphorylcholine structure of pMPC is similar to the surface structure of natural phospholipid membrane bilayers, which probably can facilitate the strong interaction between the pMPC polymer and the cellular membrane, and therefore enhance the cellular uptake.[13–15] Being bio-fouling,[11,12] which is similar to PEG, the phosphorylcholine-based polymer could replace PEGylation to be a shielding polymer for gene delivery systems. Thus, in this study, supramolecularly incorporating pMPC into the βCD-SS-P/Ad-pMPC gene carrier system could not only maintain the extracellular stability and serum tolerance, but also enhance the cellular uptake of the carrier/DNA polyplex nanoparticles, which smartly solve the "shielding dilemma" caused by the conventional PEGylation.

2.5. Delivery of Therapeutic Gene p53

The greatly enhanced overall gene transfection ability of the βCD-SS-P/Ad-pMPC pseudo-copolymer was demonstrated in delivering a therapeutic gene *p53*-encoding plasmid. The p53 gene is a tumor suppressor gene, which would inhibit cell proliferation through G1-cell cycle arrest and induce cell apoptosis.[37] Here, the p53 mRNA and p53 protein expression levels, cell cycle arrest and cell status of MCF-7 cells were evaluated after transfection with polymer/p53 polyplexes (**Figure 6**). The p53 mRNA levels of cells after transfection mediated by βCD-SS-P/Ad-pMPC were significantly higher than those of Lipofectamine, PEI 25k, βCD-P, and βCD-SS-P controls (Figure 6A). In addition, the western blotting results demonstrated that the intensity of p53 protein band of the βCD-SS-P/Ad-pMPC/p53 polyplex system was significantly higher than those of the controls, indicating that the p53 protein expressing amount was the highest for the βCD-SS-P/Ad-pMPC/p53 polyplex system due to the rational design of the carrier (Figure 6B). The cell cycle phase distributions of cells transfected by different polymer/p53 polyplexes were analyzed by flow cytometry with PI staining (Figure 6C and D). For βCD-SS-P/Ad-pMPC/p53 system, the G0/G1 phase cell population was as high as 81%. It is clear that much more cells were arrested in the G0/G1 phase and less cells were in the S phase for cells treated with the βCD-SS-P/Ad-pMPC/p53 system, as compared to all other control systems. Moreover, the percentage of apoptotic cells and dead cells induced by the polymer/p53 polyplexes were investigated by Annexin V-FITC and PI double staining (Figure 6E). The flow cytometric results demonstrated that apoptosis was

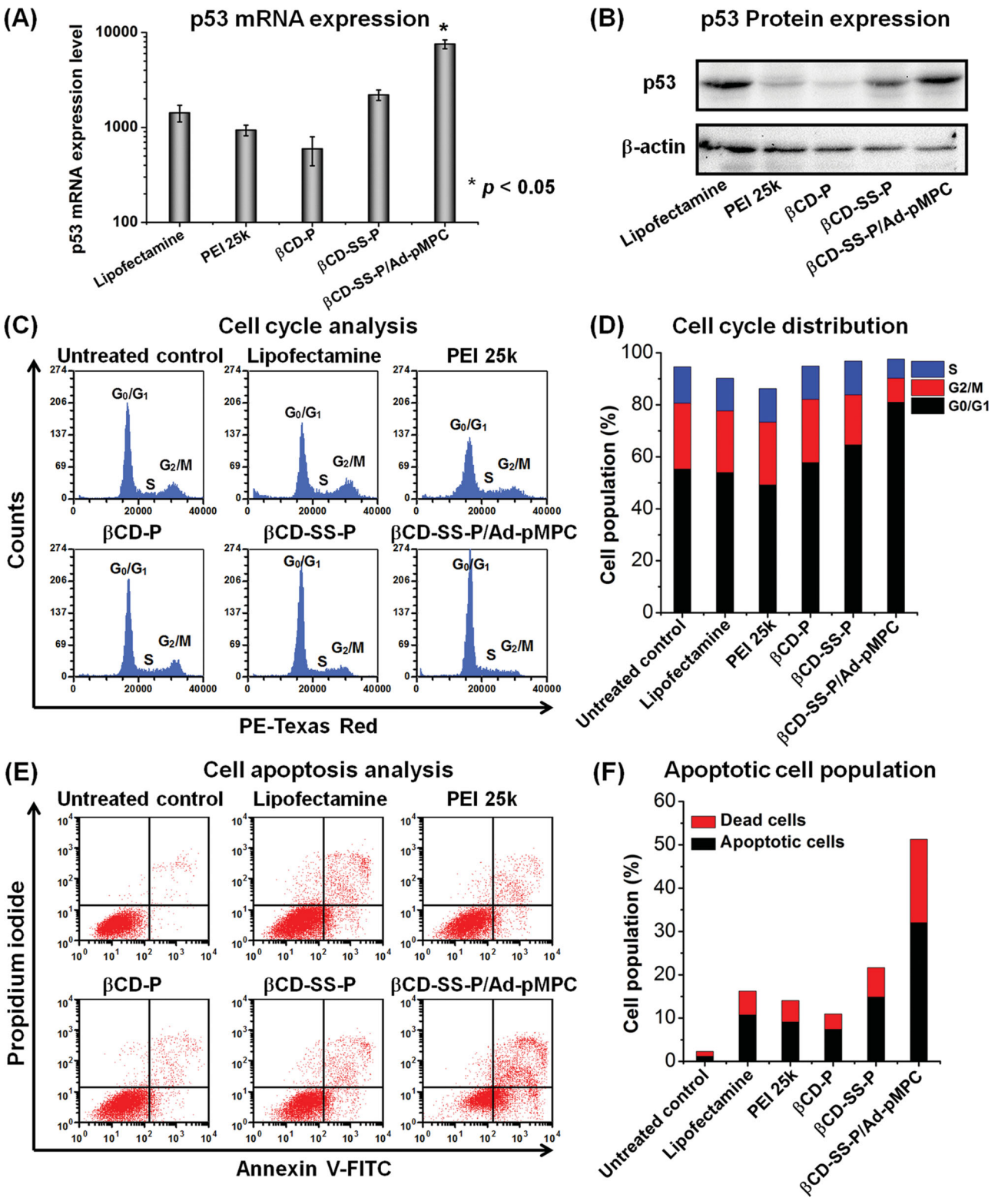

Figure 6. Delivery of p53 therapeutic gene in MCF-7 cells. A) mRNA expression levels of cells treated with polymer/p53 polyplexes. Data represent mean ± S.D. B) Western blotting analysis for p53 protein expression in cells after transfection mediated by Lipofectamine, PEI 25k, βCD-P, βCD-SS-P, and βCD-SS-P/Ad-pMPC. β-actin was used as internal control. C) Cell cycle analysis through propidium iodide (PI) staining of cells transfected with p53 polyplexes. D) Quantified cell phase distribution of cells transfected by various polymer/p53 polyplexes. E) Annexin V/PI double-staining assay of cells transfected by various polymer/p53 polyplexes. *Y*-axis shows PI labeled population and *X*-axis shows FITC-labeled Annexin V positive cells. Apoptotic cells showed a strong annexin V staining. Dead cells showed both membrane staining by annexin V and strong nuclear staining from PI. F) Population of dead and apoptotic cells induced by polymer/p53 polyplexes.

induced for 32% of the MCF-7 cells treated with βCD-SS-P/Ad-pMPC/p53 system, which was significantly higher than those of control system (Figure 6F). Thus, we could confirm that the βCD-SS-P/Ad-pMPC system possessed outstanding capacity in delivering p53 therapeutic gene.

3. Conclusions

We have prepared the star-shaped host polymer βCD-SS-P consisting of multiple arms of pDMAEMA linked to a β-CD core with bioreducible disulfide bonds, and the guest polymer Ad-pMPC being an adamantyl-end capped pMPC. The two molecular building blocks self-assembled to form a supramolecular pseudo-diblock copolymer βCD-SS-P/Ad-pMPC as a multifunctional gene carrier system with the functions of disulfide bond based reduction-responsive degradation and zwitterionic phosphorylcholine based extracellular stabilization and favorable cellular uptake for delivering DNA with significantly enhanced gene transfection efficiency. Our data showed that the formation of the supramolecular pseudo-diblock copolymer was based on the host-guest interaction between the β-CD core of the host polymer and the Ad moiety of the guest polymer. The βCD-SS-P/Ad-pMPC carrier had good DNA binding ability to form DNA polyplex nanoparticles with sizes ranging from 110 to 150 nm and zeta potential values ranging from 18 to 25 mV at N/P ratio from 10 to 40. We systematically investigated the βCD-SS-P/Ad-pMPC/DNA polyplex system in various simulated environments and MCF-7 cell culture systems under different conditions, in comparison with a number of carefully selected and designed control systems such as non-bioreducible, and non-shielding (without pMPC) or PEG shielding polyplexes. The βCD-SS-P/Ad-pMPC/DNA polyplex nanoparticles have been proved to have excellent serum stability and protein resistance due to the shielding effect of pMPC, and in the meantime showed high cellular uptake efficiency due to the membrane-mimic structure of pMPC. After the efficient cellular uptake into the cytoplasm, the polyplex nanoparticles readily released the DNA payload due to the cleavage of the disulfide bonds in the intracellular reductive environment. In addition, the βCD-SS-P/Ad-pMPC gene carrier also showed very low cytotoxicity. Therefore, the excellent protein stability, serum tolerance, cellular uptake and intracellular DNA release properties, and low cytotoxicity worked simultaneously to result in a highly efficient gene delivery system. Finally, the supramolecular βCD-SS-P/Ad-pMPC gene carrier was applied to deliver the therapeutic p53 anti-cancer gene in MCF-7 cells, and have achieved high efficiency in cell apoptosis and death, showing great potential for cancer gene therapy application.

4. Experimental Section

Formation and Characterization of βCD-SS-P/Ad-pMPC Supramolecular Pseudo-Diblock Copolymer: Solution of βCD-SS-P in deionized water was prepared with a concentration of 10 mg/mL. Determined amount of Ad-pMPC in deionized water (10 mg mL^{-1}) (mole ratio of βCD-SS-P to Ad-pMPC = 1:1) was added into βCD-SS-P solution with moderate stirring. The mixture solutions were stirred at room temperature for 24 h, followed by freeze drying. Gel permeation chromatography (GPC) analysis was carried out with a Shimadzu SCL-10A and LC-10AT system equipped with a Sephadex G-50 column (size: 2.5 cm × 32 cm), and a Shimadzu RID-10 A refractive index detector. PBS buffer solution (0.5×) was used as the eluent at a flow rate of 1.0 mL min^{-1} at 25 °C. Monodispersed poly(ethylene glycol) (PEG) standards were used to obtain a calibration curve. To confirm the formation of pseudo-block copolymer, two-dimensional nuclear overhauser effect (NOE) spectroscopy nuclear magnetic resonance (2D-NOESY NMR) was performed at 500 MHz in D_2O on a Bruker Avance DRX 500 NMR spectrometer.

Confocal Microscope Observation of Intracellular Release of DNA: MCF-7 cells were transfected by fluorescent polyplexes on MatTek 8 well chamber. After the transfection, the cells were fixed by 4% paraformaldehyde and the nuclear was stained using 2 μg mL^{-1} of DAPI for 15 min. And the cells were visualized with an Olympus FV1000 confocal laser scanning microscope (CLSM) equipped with a 100× 1.6NA oil immersion objective lens. To evaluate the intracellular distributions of DNA and carrier polymer, the ratio of colocalization of FITC labeled polymer and CX-rhodamine labeled DNA was calculated from the obtained images using ImageJ software,[38] as follows:

$$\text{polymer/DNA colocalization ratio} = F_{yellow}/F_{red} \times 100\%$$

where F_{yellow} means the yellow pixels of CX-rhodamine-DNA co-localized with FITC-polymer, and F_{red} means the red pixels of all intracellular CX-rhodamine labeled DNA. The results were expressed as means and standard deviation obtained from 20 cells at each specific time point.

Quantitative Evaluation of Intracellular DNA Release using PicoGreen Assay: To determine the amount of DNA release from βCD-SS-P/Ad-pMPC/DNA polyplex inside the cells, PicoGreen dye exclusion assay was performed. Briefly, MCF-7 cells were seeded in 12-well plates (1.5×10^5) and incubated for 20 to 24 h. Polymer/DNA polyplexes were added and the cells were incubated at 37 °C for 2 h. After determined incubation time, cells were washed with PBS twice and lysed in 200 μL of lysis buffer (1% Triton X-100 in PBS) or lysis buffer (1% Triton X-100, 2% SDS in PBS) for 30 min. Lysates were centrifuged at 15 000 *g* for 15 min at 4 °C. Then 100 μL of supernatant was mixed with diluted PicoGreen for 10 min at room temperature and then transferred to a black 96-well plate for fluorescence measurement. The fluorescence was analyzed using an FITC setting (excitation 485 nm, emission 526 nm). The percentage of released DNA of all internalized DNA is expressed by the relative fluorescence (RF), which was calculated using the following equation:

$$RF = (F_{\text{free DNA}} - F_{\text{blank}})/(F_{\text{total DNA}} - F_{\text{blank}}) \times 100\%$$

where $F_{\text{free DNA}}$ is the fluorescence induced by free DNA in the cells (sample was treated with only 1% Triton X-100), $F_{\text{total DNA}}$ is the fluorescence induced by total DNA inside the cells (sample was treated with 1% Triton X-100 and 2% SDS which could release DNA from polymer/DNA complexes), and F_{blank} is the fluorescence induced by untreated cells.

Gene Transfection of MCF-7 after D,L-buthionine sulfoximine Treatment: For investigation of transfection efficiency for cells after treatment with D,L-buthionine sulfoximine (BSO), cells were pre-treated with 500 μM of BSO solution (diluted by 20 mM stock solution in PBS) for 18 h prior to transfection. The rest procedures were the same as the transfection protocol depicted in Supporting Information.

Cell Viability of MCF-7 after BSO Treatment: For investigation of cell viability after cells were treated with BSO, cells were pre-treated with 500 μM BSO for 18 h prior to adding complexes solution. The other procedures were the same as the cell viability evaluation methods described in Supporting Information.

Effects of Serum Concentration on Transfection: The process of transfection experiments was similar to that described in Supporting Information, except that medium at the time of transfection was replaced with DMEM containing various serum concentrations (0, 5, 10, 20, 30, and 50%).

Investigation of Cellular Uptake of Polymer/DNA Polyplexes: Briefly, MCF-7 cells were seeded in 12-well plates (1.5×10^5 cells per well) and allow to attach and grow for 20 to 24 h. The cells were then incubated with the polymer/DNA polyplexes (2 μg of DNA per well, optimal N/P ratio of each sample), prepared with fluorescence labeled DNA in various FBS concentrations of DMEM medium. At different determined time, polyplex solution was removed. After the cells were washed with PBS for three times, the cells were collected and fixed in 4% paraformaldehyde. The samples were assessed by flow cytometry and confocal microscope.

Delivery of Therapeutic p53 Gene: MCF-7 cells were transfected with polyplexes containing p53-encoded plasmid. The transfection procedures were the same as those for luciferase and GFP plasmids. To measure the extent of p53 mRNA expression level upon transfection, quantitative real-time PCR technique was employed. To measure the p53 protein expression level after transfection, western blotting was performed. To monitor cell cycle arresting, MCF-7 cells were analyzed 48 h after transfection using propidium iodide staining methods. To investigate if p53 transfection induced cell apoptosis, the status of p53 transfected cells were analyzed 72 h post transfection using FITC Annexin V/Dead Cell Apoptosis Kit by flow cytometry.

Statistical Analysis: Statistical analysis was conducted using variance tests (ANOVA) with Microsoft Excel 2007. Data sets were compared using two-tailed, unpaired *t*-test. p value of < 0.05 was regarded statistically significant.

Supporting Information

Supporting Information is available from the Wiley Online Library or from the author. It includes: Synthesis and characterization of host and guest polymers; Elemental analysis of cyclodextrin and adamantyl based compounds; Biophysical properties of βCD-SS-P/Ad-pMPC supramolecular pseudo-diblock copolymer; Disintegration of particles under reductive environment; Cytotoxicity of polymer and polymer/DNA complexes; Transgene ability of polymers; Stability and protein adsorption of βCD-SS-P/Ad-pMPC/DNA polyplexes; Materials and Methods.

Acknowledgements

This work was financially supported by Agency for Science, Technology and Research (A*STAR), Singapore (SERC PSF Grant No. 102 101 0024 and JCO Grant No. 10/03/FG/06/05) and National University of Singapore (FSF Grant No. R–397–000–136–112 and R–397–000–136–731). Y.W. thanks National University of Singapore for the Graduate Scholarship.

Received: October 30, 2013
Revised: February 6, 2014
Published online: March 18, 2014

[1] M. Neu, D. Fischer, T. Kissel, *J. Gene. Med.* **2005**, *7*, 992–1009.
[2] J. M. Dang, K. W. Leong, *Adv. Drug Delivery Rev.* **2006**, *58*, 487–499.
[3] O. Boussif, F. Lezoualc'h, M. A. Zanta, M. D. Mergny, D. Scherman, B. Demeneix, J. P. Behr, *Proc. Natl. Acad. Sci. U. S. A.* **1995**, *92*, 7297–7301.
[4] X. J. Cai, C. Y. Dong, H. Q. Dong, G. M. Wang, G. M. Pauletti, X. J. Pan, H. Y. Wen, I. Mehl, Y. Y. Li, D. L. Shi, *Biomacromolecules* **2012**, *13*, 1024–1034.
[5] E. Fleige, M. A. Quadir, R. Haag, *Adv. Drug Delivery Rev.* **2012**, *64*, 866–884.
[6] S. Ganta, H. Devalapally, A. Shahiwala, M. Amiji, *J. Controlled Release* **2008**, *126*, 187–204.
[7] Y. M. Go, D. P. Jones, *Biochim. Biophys. Acta Gen. Subj.* **2008**, *1780*, 1271–1290.
[8] Z. Zhong, F. H. Meng, W. E. Hennink, *Biomaterials* **2009**, *30*, 2180–2198.
[9] G. Y. Wu, Y. Z. Fang, S. Yang, J. R. Lupton, N. D. Turner, *J Nutr* **2004**, *134*, 489–492.
[10] M. Piest, C. Lin, M. A. Mateos-Timoneda, M. C. Lok, W. E. Hennink, J. Feijen, J. F. J. Engbersen, *J. Controlled Release* **2008**, *130*, 38–45.
[11] Y. C. Chung, Y. H. Chiu, *J. Med. Biol. Eng.* **2009**, *29*, 320–324.
[12] A. L. Lewis, *Colloid Surf. B* **2000**, *18*, 261–275.
[13] H. Lomas, I. Canton, S. MacNeil, J. Du, S. P. Armes, A. J. Ryan, A. L. Lewis, G. Battaglia, *Adv. Mater.* **2007**, *19*, 4238.
[14] T. Goda, Y. Goto, K. Ishihara, *Biomaterials* **2010**, *31*, 2380–2387.
[15] M. Massignani, C. LoPresti, A. Blanazs, J. Madsen, S. P. Armes, A. L. Lewis, G. Battaglia, *Small* **2009**, *5*, 2424–2432.
[16] T. Suma, K. Miyata, Y. Anraku, S. Watanabe, R. J. Christie, H. Takemoto, M. Shioyama, N. Gouda, T. Ishii, N. Nishiyama, K. Kataoka, *ACS Nano* **2012**, *6*, 6693–6705.
[17] H. Lee, A. K. R. Lytton-Jean, Y. Chen, K. T. Love, A. I. Park, E. D. Karagiannis, A. Sehgal, W. Querbes, C. S. Zurenko, M. Jayaraman, C. G. Peng, K. Charisse, A. Borodovsky, M. Manoharan, J. S. Donahoe, J. Truelove, M. Nahrendorf, R. Langer, D. G. Anderson, *Nat. Nanotechnol.* **2012**, *7*, 389–393.
[18] E. Mastrobattista, M. van der Aa, W. E. Hennink, D. J. A. Crommelin, *Nat. Rev. Drug Discovery* **2006**, *5*, 115–121.
[19] P. K. Lo, P. Karam, F. A. Aldaye, C. K. McLaughlin, G. D. Hamblin, G. Cosa, H. F. Sleiman, *Nat. Chem.* **2010**, *2*, 319–328.
[20] L. C. Yin, Z. Y. Song, Q. H. Qu, K. H. Kim, N. Zheng, C. Yao, I. Chaudhury, H. Y. Tang, N. P. Gabrielson, F. M. Uckun, J. J. Cheng, *Angew. Chem. Int. Ed.* **2013**, *52*, 5757–5761.
[21] D. Harries, D. C. Rau, V. A. Parsegian, *J. Am. Chem. Soc.* **2005**, *127*, 2184–2190.
[22] Z. X. Zhang, K. L. Liu, J. Li, *Macromolecules* **2011**, *44*, 1182–1193.
[23] Z. X. Zhang, X. Liu, F. J. Xu, X. J. Loh, E. T. Kang, K. G. Neoh, J. Li, *Macromolecules* **2008**, *41*, 5967–5970.
[24] Y. Ping, C. D. Liu, Z. X. Zhang, K. L. Liu, J. H. Chen, J. Li, *Biomaterials* **2011**, *32*, 8328–8341.
[25] M. E. Davis, J. E. Zuckerman, C. H. J. Choi, D. Seligson, A. Tolcher, C. A. Alabi, Y. Yen, J. D. Heidel, A. Ribas, *Nature* **2010**, *464*, 1067-U1140.
[26] Y. Ping, Q. Hu, G. Tang, J. Li, *Biomaterials* **2013**, *34*, 6482–6494.
[27] A. Harada, R. Kobayashi, Y. Takashima, A. Hashidzume, H. Yamaguchi, *Nat. Chem.* **2011**, *3*, 34–37.
[28] H. Yamaguchi, Y. Kobayashi, R. Kobayashi, Y. Takashima, A. Hashidzume, A. Harada, *Nat. Commun.* **2012**, *3*.
[29] M. E. Davis, M. E. Brewster, *Nat. Rev. Drug Discovery* **2004**, *3*, 1023–1035.
[30] O. Peters, H. Ritter, *Angew. Chem. Int. Ed.* **2013**, *52*, 8961–8963.
[31] H. W. Zhang, S. V. Vinogradov, *J. Controlled Release* **2010**, *143*, 359–366.
[32] O. M. Merkel, R. Urbanics, P. Bedocs, Z. Rozsnyay, L. Rosivall, M. Toth, T. Kissel, J. Szebeni, *Biomaterials* **2011**, *32*, 4936–4942.
[33] H. Lomas, J. Z. Du, I. Canton, J. Madsen, N. Warren, S. P. Armes, A. L. Lewis, G. Battaglia, *Macromol. Biosci.* **2010**, *10*, 513–530.
[34] S. Tu, Y. W. Chen, Y. B. Qiu, K. Zhu, X. L. Luo, *Macromol. Biosci.* **2011**, *11*, 1416–1425.
[35] S. Mishra, P. Webster, M. E. Davis, *Eur. J. Cell. Biol.* **2004**, *83*, 97–111.
[36] J. Bai, Z. Y. Zhou, H. L. Tang, S. X. Song, J. L. Peng, Y. H. Xu, *J. Liposome Res.* **2013**, *23*, 1–10.
[37] L. L. Nielsen, D. C. Maneval, *Cancer Gene Ther.* **1998**, *5*, 52–63.
[38] Y. Wen, Z. Guo, Z. Du, R. Fang, H. Wu, X. Zeng, C. Wang, M. Feng, S. Pan, *Biomaterials* **2012**, *33*, 8111–8121.